

## Research Article

# Laser Surface Alloying of 316L Stainless Steel with Ru and Ni Mixtures

M. B. Lekala,<sup>1</sup> J. W. van der Merwe,<sup>1</sup> and S. L. Pityana<sup>2</sup>

<sup>1</sup> School of Chemical and Metallurgical Engineering, University of the Witwatersrand and DST/NRF Centre of Excellence in Strong Materials, Johannesburg 2001, South Africa

<sup>2</sup> Council for Scientific and Industrial Research, National Laser Centre, Pretoria 0001, South Africa

Correspondence should be addressed to J. W. van der Merwe, josias.vandermerwe@wits.ac.za

Received 14 March 2012; Accepted 22 May 2012

Academic Editor: Muthukannan Duraiselvam

Copyright © 2012 M. B. Lekala et al. This is an open access article distributed under the Creative Commons Attribution License, which permits unrestricted use, distribution, and reproduction in any medium, provided the original work is properly cited.

The surfaces of AISI 316L stainless steel were laser alloyed with ruthenium powder and a mixture of ruthenium and nickel powders using a cw Nd:YAG laser set at fixed operating parameters. The microstructure, elemental composition, and corrosion characteristics of the alloyed zone were analyzed using optical and scanning electron microscopy (SEM), energy dispersive X-ray spectroscopy (EDX), and corrosion potential measurements. The depth of alloyed zone was measured using the AxioVision program and found to be approximately 1.8 mm for all the alloyed specimens. Hardness profile measurements through the surface-substrate interface showed a significant increase from 160 HV for the substrate to a maximum of 247 HV for the alloyed layer. The sample laser alloyed with 80 wt% Ni-20 wt% presented the most noble corrosion potential ( $E_{\text{corr}}$ ) of  $-0.18$  V and the lowest corrosion current density ( $i_{\text{corr}}$ ).

## 1. Introduction

Minor additions of ruthenium to the bulk volume of steels resulted in a significant improvement of corrosion resistance in many reducing environments [1]. Ruthenium modified alloys possesses properties which render them candidate alloys to replacing the expensive nickel-based alloys which are currently used in more aggressive corrosion environments [2]. However, owing to the high-cost associated with ruthenium, bulk alloying is currently not a feasible means, although opportunities to explore the method exist. For instance, Streicher [3] observed a synergistic benefit when ruthenium and nickel were added together to steels. This observation offers an opportunity to reduce the amount of ruthenium per bulk volume added in the alloying process, yet presents significant improved corrosion resistance. Thus, minor additions of ruthenium together with nickel present an economically sound approach of modifying corrosion properties of alloys. Furthermore, since corrosion is a surface phenomenon, an equally cost-effective approach is to add these only on the surface, where protection is most required.

Laser surface modification techniques have been extensively studied for selective improvement of surfaces for wear,

hardness, and corrosion [4–7]. The laser surface alloying technique is particularly applicable in cases where a change in the chemical composition and microstructure of the surface is required. The laser surface alloying technique enables external alloying elements to be added into the bulk material via a laser generated melt pool. Generally, the external alloy material is either preplaced on the desired surface of the substrate or fed into the melt pool. The alloy material reacts with the molten surface to create a new alloyed layer which exhibits unique properties, such as high corrosion resistance. Studies of corrosion resistance on laser surface alloyed of ferritic Fe-40Cr alloy with ruthenium (Ru) showed improvement when subjected to certain corrosive environments [8]. Despite these beneficial results, surface modification of alloys with ruthenium (Ru) to improve their corrosion properties has received little attention. In South Africa, there has been a renewed interest in investigating the effects of adding small amounts of Ru metals for improving corrosion resistance of stainless steels. It has been established that small additions of Ru in the steel shifts the corrosion potential to more noble values [1]. Streicher [3] pointed out that addition of Ni also has potential benefits.

TABLE 1: Composition of the powders used on sample.

Alloy name	Powder composition		Substrate material
	Nickel wt%	Ruthenium wt%	
Alloy 1	0	100	AISI 316
Alloy 2	80	20	AISI 316
Alloy 3	50	50	AISI 316

In this study, laser surface alloying of AISI 316 with Ru and with (Ru + Ni) mixed powders was investigated. The effect of the amounts of Ru added into the alloyed layer was studied by selecting a mixture with the following compositions (80 wt% Ni + 20 wt% Ru) and (50 wt% Ni + 50 wt% Ru). The objective(s) has been to keep the Ru content low, while maintaining superior corrosion resistance. The microstructure, chemical composition, hardness, and corrosion behaviour of the alloyed layers were analysed using SEM, EDX, hardness tester, and corrosion potentials.

## 2. Experimental Details

**2.1. Laser Surface Alloying.** The AISI 316 stainless steel was cut into  $10 \times 5 \times 0.5$  cm rectangular plates. The surfaces of the plates were sandblasted and cleaned with acetone prior to laser surface alloying. Nickel and ruthenium were in the form of powders of commercial purity, 99.6 wt% and 99.9 wt%, respectively, were used to surface alloy AISI 316 stainless steel samples. The powders were mixed to specific Ru: Ni wt% proportions, and Table 1 shows the powder weight ratios used on each sample. The mixed powders were preplaced on the steel surface using a chemical binder. The thickness of the preplaced powder coatings could be controlled to approximately 1 mm.

The laser surface alloying was performed with a Rofin Sinar DY044 continuous wave Nd: YAG laser. A  $600 \mu\text{m}$  optical fibre was used to guide the laser beam to the laser processing head. The processing head was mounted on a KUKA's articulated robot arm. The laser head was set at a fixed distance of 12 mm above the substrate. The laser process parameters were kept the same for all samples. The laser power, beam diameter, and scan speed were 4 kW, 4 mm, and 0.8 m/s, respectively. These parameters were chosen after a number of experimental tests done to establish acceptable alloys. Large coated areas were made by parallel tracks overlapped by 2 mm. The whole laser surface alloying operation was carried out in an inert argon environment to prevent oxidation.

**2.2. Material Characterization.** Metallographic specimens were prepared by cutting the samples transversally across the alloyed layer and mounting the pieces separately in a bakelite or/and lucite powder using a mounting press. The samples were etched electrolytically in 60 wt% nitric acid in distilled water at 1.5 V for 20 s. The microstructures and the elemental composition profile were evaluated using Zeiss Axiotech 25 HD microscope and JSM 5800 LV SEM with energy dispersive X-ray spectroscopy (EDS), respectively.

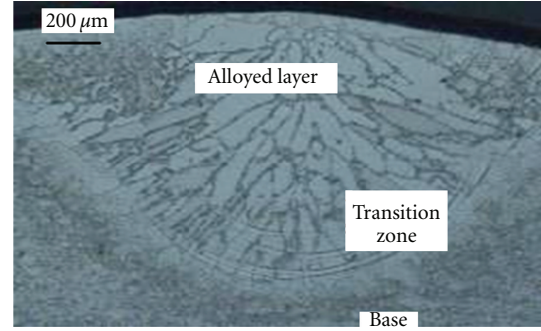


FIGURE 1: Typical cross section of the laser alloyed zone.

The hardness was determined using a Future-Tech FM-700 Vickers Micro-hardness testing instrument.

**2.3. Electrochemical Tests.** The corrosion tests were carried out in 80% sulphuric acid solution which was kept at  $60^\circ\text{C}$  using a thermostat-controlled bath. The corrosion performance of the laser alloyed surfaces was evaluated by means of electrochemical polarization measurements using an Autolab potentiostat, which utilizes platinum as the opposite electrode and a saturated silver-silver chloride electrode as the reference electrode. Potentiodynamic polarization curves were obtained for each alloy. A scanning rate of 0.1 mV/sec was used to conduct all the measurements.

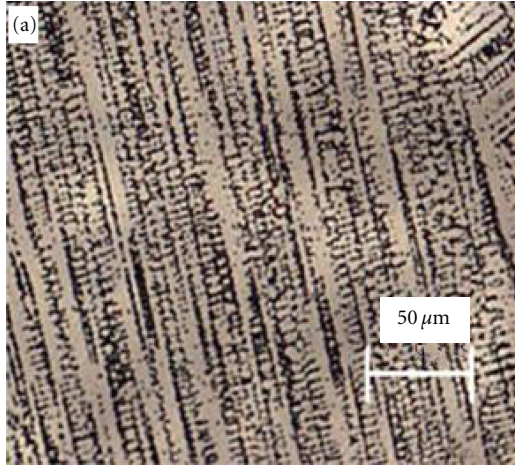
## 3. Results and Discussion

**3.1. Microstructure of the Laser Alloyed Layers.** Figure 1 shows an optical micrograph of the cross sectional view of Alloy 1; sectioned perpendicular to the scanning direction. The width and depth of the cross section were approximately 4 mm and 1.8 mm, respectively. The alloyed zone was free of cracks and pores. The cross section showed three distinct regions: the alloyed layer, the transition zone and heat affected zone. The microstructure in the alloyed zone showed columnar grains which are attributed to rapid melting and directional solidification. Similar cross sections were obtained for the other alloys.

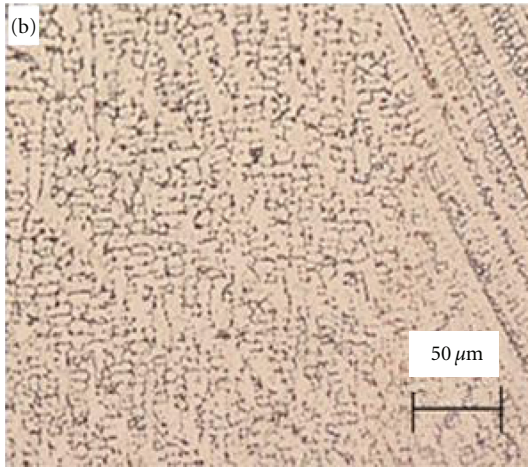
Figure 2 shows high magnification optical micrographs of alloys 1 and 2. The microstructure of alloy 1 shown in Figure 2(a), consisted of dendritic microstructures, while that of alloy 2 (Figure 2(b)) showed both dendrites and columnar grains of different orientations. This confirms that grain growth took place in preferential directions. The microstructures in Figure 2 are typical of weld beads which cooled under nonequilibrium conditions [9]. The ruthenium distribution was homogenous throughout the weld bead.

The average chemical composition of the laser alloyed layer obtained by EDX analysis is shown in Table 2. The elemental composition of the alloyed layer is consistent with the alloying material. The alloying material was melted and dissolved into the base material.

**3.2. Microhardness.** Microhardness measurements across the bead-substrate interface revealed a significant increase in



(a)



(b)

FIGURE 2: Optical microstructures of laser alloyed AISI 316 SS: (a) alloy 1 (9.6% Ru) and (b) alloy 2 (5.6% Ru).

TABLE 2: EDX elemental composition of the laser alloyed layer (wt%) with an error of 0.2 wt%.

Alloys	Al	Si	Cr	Mn	Fe	Ni	Mo	Ru
Alloy 1	0.1	0.4	16.2	1.6	61.2	9.1	1.8	9.6
Alloy 2	0.1	1.3	17.1	1.3	50.3	22.8	1.5	5.6
Alloy 3	0.1	1.2	14.7	1.3	53.5	16.9	1.0	9.5

hardness, varying from 158 HV for the AISI 316 to substrate 247 HV for the laser alloyed bead, for alloy 1, Figure 3. The increased hardness of alloys 1 and 2 can be attributed to their high Ru and Ni content, as well as the microstructural changes due to laser heating. The hardening effect of both ruthenium and nickel on alloys is well-known [10].

3.3. *Potentiodynamic Polarization Behaviour.* Potentiodynamic polarisation curves of the samples tested in 80% sulphuric acid at 60°C are shown in Figure 4. Although all samples exhibited passivation, there was a level of instability associated with the passive layer that formed on the bare

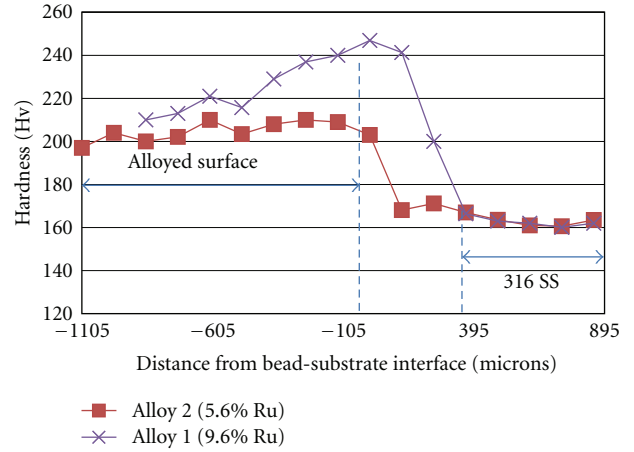


FIGURE 3: Variation of hardness with the distance from the bead/substrate interface in an AISI 316 stainless steel surface alloyed with Ru. The hardness measurements showed an error of approximately 3%.

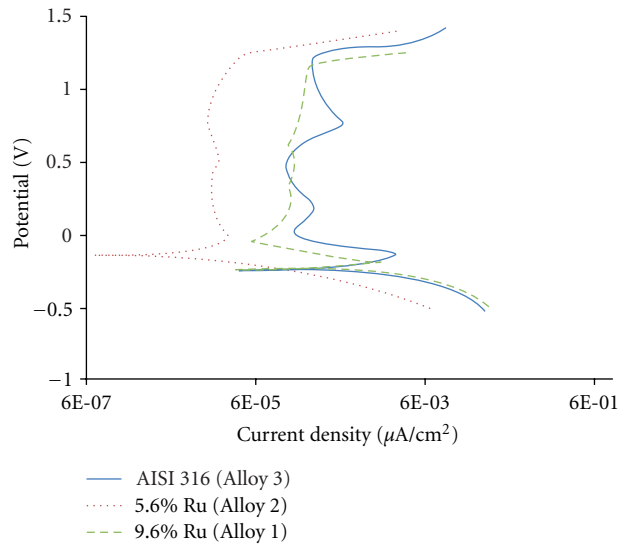


FIGURE 4: Comparison of potentiodynamic polarization curves for AISI 316 SS substrate, 5.6 wt% Ru steel and 9.6 wt% Ru steel.

substrate material. The bare substrate and the 9.6 wt% Ru surface corroded at similar corrosion potentials ( $E_{corr}$ ) and they both passivated at comparable current densities,  $i_{pass}$ . The passive region of the 5.6 wt% Ru sample, indicated that anodic reaction was inhibited with the enhancement of polarization potential. In addition, it can be seen from Figure 4 that the 5.6 wt% Ru sample exhibited the noblest corrosion potential ( $E_{corr}$ ) with a value of  $-0.18$  V and the lowest corrosion current density ( $i_{corr}$ ) with a value of approximately  $5 \times 10^{-5}$  A/cm<sup>2</sup>. Conversely, the substrate showed the lowest  $E_{corr}$  with a value of  $-0.25$  V and the highest  $i_{corr}$  with a value of  $1 \times 10^{-3}$  A/cm<sup>2</sup>, which suggested that the 5.6 wt% Ru alloy exhibited the best anticorrosive properties. Despite its higher Ru content, alloy 1 showed less improvement on the corrosion properties of AISI 316 SS



than alloy 2. The better corrosion properties of alloy 2 can be attributed to the higher nickel content. On the other hand, the presence of undissolved Ru particles in alloy 1 is a sign of poor alloying and most likely led to poor corrosion properties. The results show that the nature of the microstructure and other alloying elements such as Ni play a vital role on the influence of Ru on corrosion properties of steels. Higher nickel content enhanced the influence of Ru. This phenomenon has been observed by Steicher [3] and Higginson [11], although at lower concentrations of less than 0.5 wt% Ru.

#### 4. Conclusions

Higher Ru content on the surface does not necessarily give better corrosion behavior. The effect of Ru on the corrosion behavior of the surface depended on the amount of Ni present. Higher nickel contents showed more effective improvements in corrosion resistance. Thus, laser surface alloying with Ru and Ni together present an economical way of using the two elements, because the Ru amount can be kept optimally low for maximum corrosion enhancement. The nature of the alloyed surface was greatly affected by the variation in the composition of the preplaced powder, thus showing that the laser surface alloying is system dependent. Further investigations into the surface alloying with ruthenium and nickel, particularly to identify their optimal composition for maximum corrosion improvements on various steel surface, is highly recommended. The laser surface alloying with Ru and nickel can be applied to various alloys. The surface alloying approach might be particularly suitable for thick engineering components or plates which require better corrosion properties, although the alloying should be sufficient to ensure that all the elements are in solution.

#### Acknowledgments

The authors would like to thank the CSIR-National Laser Centre for using its facilities. The Department of Science and Technology and the National Research Foundation, South Africa, are thanked for funding and support.

#### References

- [1] J. H. Potgieter, A. M. Heyns, and W. Skinner, "Cathodic modification as a means of improving the corrosion resistance of alloys," *Journal of Applied Electrochemistry*, vol. 20, no. 5, pp. 711–715, 1990.
- [2] P. A. Olubambi, J. H. Potgieter, and L. Cornish, "Corrosion behaviour of superferritic stainless steels cathodically modified with minor additions of ruthenium in sulphuric and hydrochloric acids," *Materials and Design*, vol. 30, no. 5, pp. 1451–1457, 2009.
- [3] M. A. Streicher, "Development of pitting resistant Fe-Cr-Mo alloy," *Corrosion*, vol. 30, no. 3, pp. 77–91, 1974.
- [4] L. A. B. Mabwali, S. L. Pityana, and N. Sacks, "Laser surface alloying of aluminum (AA1200) with Ni and SiC powders," *Materials and Manufacturing Processes*, vol. 25, no. 12, pp. 1397–1403, 2010.
- [5] L. Mabwali, S. Pityana, and N. Sacks, "Laser alloying of Al with mixed Ni, Ti and SiC powders," *Journal of Laser Applications*, vol. 22, no. 4, pp. 121–126, 2010.
- [6] S. Anandan, L. Pityana, and J. Dutta Majumdar, "Structure-property-correlation in laser surface alloyed AISI 304 stainless steel with WC + Ni + NiCr," *Materials Science and Engineering A*, vol. 536, pp. 159–169, 2012.
- [7] J. D. Majumdar and I. Manna, "Laser surface alloying of AISI 304-stainless steel with molybdenum for improvement in pitting and erosion-corrosion resistance," *Materials Science and Engineering A*, vol. 267, no. 1, pp. 50–59, 1999.
- [8] S. C. Tjong, J. S. Ku, and N. J. Ho, "Laser surface alloying of ferritic Fe-40Cr alloy with ruthenium," *Surface and Coatings Technology*, vol. 90, no. 3, pp. 203–209, 1997.
- [9] R. W. K. Honeycombe and H. K. D. H. Bhadeshia, *Steels: Microstructure and Properties*, Butterworth-Heinemann, Oxford, UK, 2nd edition, 1995.
- [10] C. A. Hampel, *Rare Metals Handbook*, New York, NY, USA, 1954.
- [11] A. Higginson, *The passivation of Fe-Cr-Ru alloys in acidic solutions [Ph.D. thesis]*, University of Manchester, 1987.